Chapter 9
Dosimetry of Laser-Driven Electron Beams for Radiobiology and Medicine

Luca Labate, Debora Lamia and Giorgio Russo

Abstract In this chapter, the main issues related with the usage of "standard" dosimetric methods for the characterization of laser-driven electron beams will be discussed. In particular, an overview of the main devices used for the characterization of electron beams used in medical applications will be given. The issues possibly arising in the usage of techniques established for conventional accelerators for the dosimetry of ultrashort laser-driven beams will also be given.

9.1 Introduction

In order for laser-driven electron accelerators to be used for applications in the field of radiotherapy, the capability of performing both absolute and relative dosimetry on the electron beam is an essential prerequisite. From a general point of view, a dosimetric characterization would be aimed at maximizing the dose delivered to the cancer cells while, at the same time, keeping the dose to the neighbour tissues as low as possible. This also involves a detailed characterization of the primary beam, in terms, for instance, of its energy and spatial features.

It is worth noticing, at this point, that, while already providing electron bunches with the main figures very similar to those delivered by typical LINAC-based machines employed in the radiotherapy practice [1–3], a laser-driven accelerator exhibits peculiar features as for some important parameters. As an example, Table 9.1 shows a few parameters for the electron bunches delivered by one of the

L. Labate (✉)
Istituto Nazionale Di Ottica, Consiglio Nazionale Delle Ricerche, Pisa, Italy
e-mail: luca.labate@ino.it

D. Lamia · G. Russo
Istituto Di Bioimmagini E Fisiologia Molecolare, Consiglio Nazionale Delle Ricerche, Cefalù, Italy
e-mail: debora.lamia@ibfm.cnr.it

G. Russo
e-mail: giorgio.russo@ibfm.cnr.it

A. Giulietti (ed.), *Laser-Driven Particle Acceleration Towards Radiobiology and Medicine*, Biological and Medical Physics, Biomedical Engineering, DOI 10.1007/978-3-319-31563-8_9

Table 9.1 Main parameters of the electron bunches delivered by an IOERT machine as compared with the ones by a possible laser-driven machine

Parameter	LIAC ®	Laser-driven
Max e^- energy	12 MeV	up to ∼100 MeV
Charge per bunch/shot	1.8 nC	1 nC
Repetition rate	5–20 Hz	10 Hz
Average current	18 pA (@10 Hz)	10 pA
Bunch duration	∼1 μs	∼1 ps
Peak current	∼1 mA	<1 kA
Instantaneous dose rate	$\sim 10^7$ Gy/s	$\sim 10^{12}$–10^{13} Gy/s

The LIAC machine is produced by Sordina IORT Technologies S.p.A. (see [8])

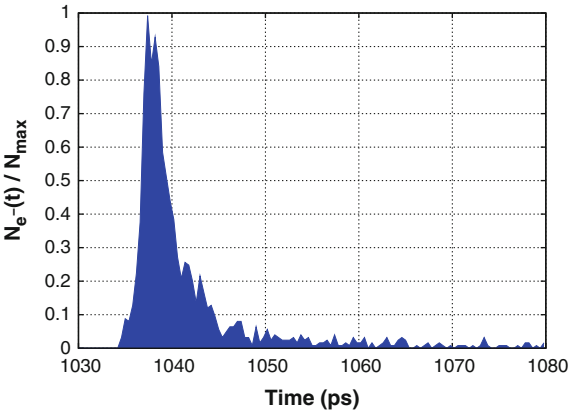

Fig. 9.1 Monte Carlo simulation (performed using the GEANT4 toolkit) of the arrival times of electrons reaching the position of an hypothetic cell sample in a typical situation encountered in a laser-driven accelerator (see text). Time $t = 0$ corresponds to the electrons leaving the acceleration region (i.e., the plasma). The width of the curve basically gives an estimate of the electron bunch lengthening due to scattering processes along the transport line

LINAC-based machines currently most employed for the so-called Intra-Operative Electron Radiation Therapy (IOERT), as compared to the same parameters of a bunch from a possible laser-driven machine. Looking at the table, it is clear that a laser-driven accelerator features an electron bunch duration much smaller than a conventional acclerator. For instance, Fig. 9.1 shows the distribution of the arrival times of the electrons on an hypothetical patient after having propagated through a collimating tube 60 cm long and having crossed a 60 μm thick brass vacuum window. In the simulation providing the result shown in the Figure (where no account was made of Coulomb or energy dispersion bunch lengthening) all the primary electrons were considered to leave the gas-jet at the same time ($t = 0$). Thus the curve shown would actually have to be considered as a transfer curve to be convolved with the actual bunch duration in order to get the final bunch time

profile. However, since durations of a few up to a few tens of femtoseconds have been reported for the bunches on leaving the plasma [4], a bunch duration of a few picoseconds can be safely estimated/calculated at the position of the biological tissue or patient (that is, generally speaking, after a few tens of centimeters propagation and a vacuum-air interface). This figure is still about six orders of magnitude smaller than that of a typical LINAC used in radiotherapy. By taking into account the typical bunch charge in the two cases (which is more or less comparable), one can easily realize that a much higher instantaneous dose rate is actually obtained, whose biological consequences have still to be investigated in depth. Further differences of a laser-driven acclerator when compared to a conventional one rely on the broader energy spectrum (when no advanced injection schemes are implemented, such as in the typical case of a tentatively "ease-to-use" accelerator for medicine) and, in general, a higher divergence (see, for instance, [5] for a discussion of the typical spectral features encountered in an IOERT machine or [6] for a general discussion of LINAC-based accelerators for medicine).

Besides to possibly leading to new processes occurring at the biological level (see for instance [7]), the above arguments make thus clear that attention has to be paid when using standard techniques, well consolidated into the clinical practice, to carry out dosimetry of laser-driven electron bunches. In this chapter we briefly give an overview of the methods and devices currently used in medical dosimetry; the issues related with the extension of such techniques to laser-driven bunches will be highlighted.

9.2 Absolute and Relative Dosimetry of Laser-Driven Beams

As said above, many medical applications, such as radiotherapy or nuclear medicine, require a precise knowledge of the absolute dose released from ionizing radiation. In fact, the capability to carry out absolute dosimetry of a radiation treatment is a necessary prerequisite to estimate the planned dose with respect to the delivered dose.

The international dosimetry protocols recommend appropriate procedures to be followed and specific detectors to be used for high energy photon and particle beams generated by clinical accelerators [9–11]. An uncertainty higher than 5 % in the absorbed dose evaluation jeopardize the effectiveness of treatment and the patient's health. For instance, the IAEA code of practice [9] for dosimetric measurements in radiotherapy with electron beams recommends to place the ionization chamber in water. Furthermore, the usage of a plane-parallel ionization chamber is recommended for electron beams with energy ≤10 MeV, whereas the usage of cylindrical chambers is required for electron beams with energy above 10 MeV. Moreover, the code of practice [9] specifies the reference conditions for determining the absorbed dose by electron beams. Any issue potentially affecting the

measurement must be taken into account, such as the geometric arrangement (distance and depth which the ionization chamber is placed at), the size of the radiation field, the material and the size of the irradiated phantom, the environment temperature and pressure. The set of values of the above quantities chosen for the ionization chamber calibration defines the reference conditions. The main parameter used as the electron beam quality index and used to obtain the reference conditions is the R_{50}. This physical quantity is the depth in water, expressed in $\mathrm{g/cm^2}$, where the absorbed dose is 50 % of the maximum in the Percentage Depth Dose curve (PDD curve). While for any R_{50} value the reference phantom material is water, for $R_{50} < 4\,\mathrm{g/cm^2}$ plastic phantoms can also be used. Moreover, for $R_{50} \geq 4\,\mathrm{g/cm^2}$ the measurements can be carried out using either plane-parallel or cylindrical ionization chambers; for $R_{50} < 4\,\mathrm{g/cm^2}$ the use of plane-parallel chambers is suggested only. The position of the reference point of the plane-parallel ionization chamber is given by $z_{ref} = 0.6\,R_{50} - 0.1\,\mathrm{g/cm^2}$. For a cylindrical chamber, the position of the reference point is $0.5 r_{cyl}$ beyond z_{ref}, being r_{cyl} the internal radius of the chamber cavity. The source-surface distance (SSD), that is the distance from the source to the surface of the patient or of the phantom, is 100 cm. Finally, the field size at the phantom surface suggested by IAEA TRS-398 is at least $10 \times 10\,\mathrm{cm}$ for $R_{50} \leq 7\,\mathrm{g/cm^2}$ and at least $20 \times 20\,\mathrm{cm}$ for $R_{50} > 7\,\mathrm{g/cm^2}$. Suitable correction factors to the measured charge are also to be taken into account, should the experimental conditions differ from those of calibration of the ionization chamber. The absorbed dose in water D_w in non-reference conditions can be calculated as

$$D_w = N_D M \sum_i k_i \tag{9.1}$$

where N_D is a calibration factor depending on the dosimeter, M is the physical quantity measured by the electrometer and k_i is the ith correction factor. In particular, the correction factors to be used are:

- k_{X,X_0}: if the ionization chamber has been calibrated with a beam with quality X and the experimental measurement has been carried out with a beam with a different quality X_0;
- k_{Tp}: this correction factor takes into account the different values of temperature and pressure with respect to the reference conditions;
- k_S: this is a factor aimed at correcting the response of an ionization chamber for the lack of complete charge collection due to ion recombination in the sensitive volume;
- k_{pol}: this correction factor is used when a change of the sign of the polarizing voltage applied to the chamber has to be accounted for;
- k_{elec}: this is a specific calibration factor of an electrometer.

To date, no dosimetric protocols have been established for absolute dosimetry of laser-driven electron beams, due to the very high instantaneous dose rate of these beams. Indeed, as said above, a typical laser-driven accelerator delivers electron

beams with a few tens of fs up to a few ps duration; such figure is about six orders of magnitude shorter than for a typical LINAC used in radiotherapy (see [6] and references therein). In the remaining of this section we provide an overview of the different types of detectors which can be used to get either absolute or relative dosimetry of laser-driven particle beams.

9.2.1 Radiochromic Films

The radiochromic films, perhaps the most used detectors in the field of laser-driven electron acceleration, represents a class of self-developing detectors whose response is independent of the dose per pulse; as it is well known, if exposed to radiation, they blacken proportionally to the received dose. The change in the optical density is direct and does not require any chemical treatment. Radiochromic films based on polydiacetylene (PDA), a family of conductive polymers, have been introduced especially for medical applications [12], generally referred to as Gafchromic. The relationship between optical absorbance and absorbed dose by Gafchromic films can be considered semilinear [13]. Different types of Gafchromic films are available, whose usage is chosen according to the application (see for instance [14]). For instance, in the context of radiodiagnostics, Gafchromic XR-M2 films (Fig. 9.2) are used for mammography quality assurance testing; they allow the light field and the radiation field to be measured. In the same context, Gafchromic XR-CT2 films (Fig. 9.3) are designed for the measurement of radiation beam slice width on Computed Tomography (CT) scanners in real time. EBT3 Gafchromic films (Fig. 9.4) are used in radiotherapy for dosimetric measurements; the structure of these films is symmetric and they do not require post-exposure processing [15].

Gafchromic films have a fast time response, are independent on the value of dose per pulse and exhibit a low response dependence on the electron energy. For these reasons, these detectors are well suited to reveal the dose delivered by a laser-driven

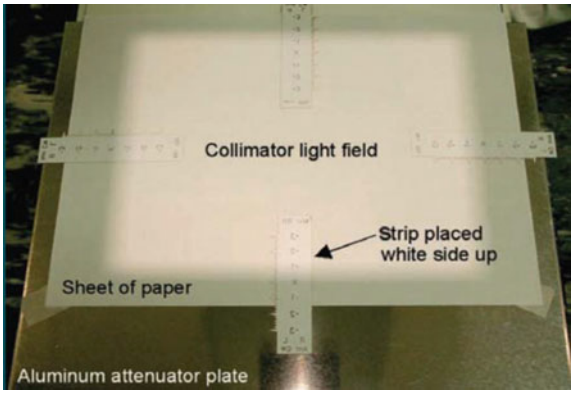

Fig. 9.2 Example of an XR-M2 Gafchromic film. A single film can be used to define the relative positions of the light field and of the radiation field for quality assurance in mammography

Fig. 9.3 Esample of an XR-CT2 Gafchromic film. Such a film can be used to measure the beam width of a CT scanner in real time

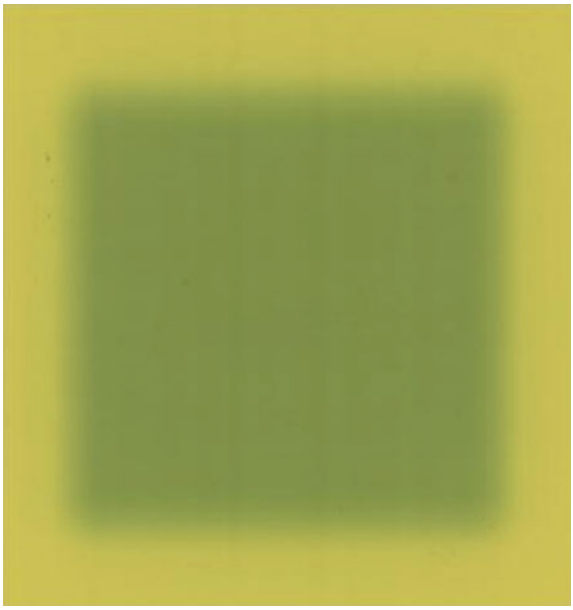

Fig. 9.4 Example of a typical electron signal on an EBT3 type gafchromic film, used for dosimetric measurements in radiotheraphy

accelerator. In particular, due to the dosimetric features similar to the accelerators used in radiotherapy, the use of the EBT3 films is mostly appropriate.

In order to account for possible slight differences in the response of each sample, the films may be calibrated with a clinical commercial accelerator. For example, if the laser-driven accelerator generates electron beams, the gafchromic films can be calibrated by an accelerator used for clinical treatment of intraoperative radiotherapy (IORT) [16]. The calibration allows a curve of dose as a function of the intensity of each pixel as gained by a film scan (see for instance Fig. 9.5).

One of the most useful features of Gafchromic films is their ability to be arranged in such a way as to obtain 3D maps of the deposited dose. For instance, suitable arrangements and subsequent analysis of gafchromic films allows the dose as a function of depth, the Percentage Depth Dose (PDD) curve, the 3D dose maps and two-dimensional dose distributions to be retrieved [16]. Moreover, the radiochromic films allow the analysis of the homogeneity and symmetry of the spatial distribution of the dose through the transverse profile of the beam [17]. It is worth reminding, at this point, that for the sake of a definition of the final expected performances of an

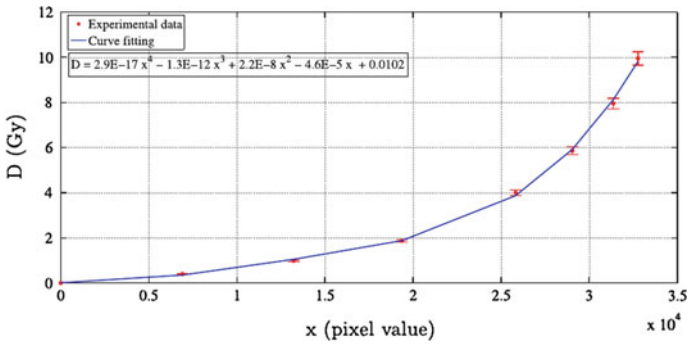

Fig. 9.5 Example of a calibration curve of EBT3 films, showing the relationship between the absorbed dose and the value of the pixel intensity as read from a film scan. Figure credit: [16]

accelerator, the code of practice for intraoperative radiation therapy using mobile electron linear accelerators [10] recommends flatness and symmetry checks monthly with a tolerance of 3 % and annually with a tolerance of 2 %.

9.2.2 Ionization Chambers

The ionization chamber is a gas-filled detector which is based on the detection of direct ionization created by the passage of the radiation. A charged particle passing through a gas, can excite or ionize the gas molecules that encounters in its path. The application of an electric field in the ionization chamber allows to collect all the charges created by the ionization of the gas. The number of ion pairs created along the track of the radiation is the measurement provided by the chamber. Because of the possible recombination processes of charged particle pairs that take place inside the cavity of the ionization chamber, it is evident that the charge separation and collection must occur in a very short time. This is the reason why the application of intense electric fields is recommended. Figure 9.6 shows the different operating regimes of a generic gas detector. The range of values of the voltage applied to the electrodes of the ionization chamber, 100–1000 V, defines the so-called saturation region in which the ionization chambers operate; in this area the number of ions collected at the electrodes per unit of time is constant.

The application of an electric field between the two electrodes ensures that positive ions have a drift velocity in the direction of the electric field, while electrons and negative ions in the opposite direction. Typical harvest times for the electrons are on the order of μs, instead of ms as in the case of ions. The dosimetric international protocols [9, 11] states that in cases of accelerators with high dose rate ($>$ cGy/pulse), the reference dosimetry using an ionization chamber cannot be

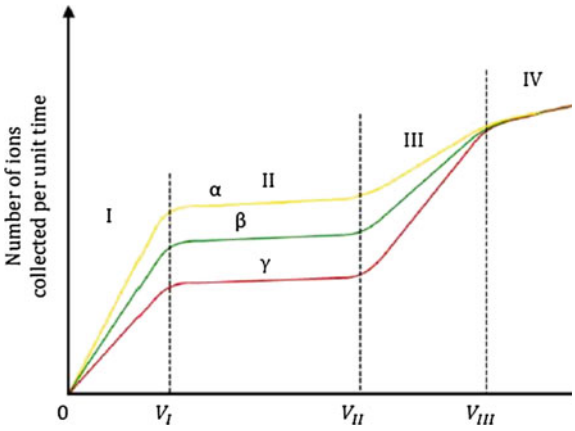

Fig. 9.6 Typical behaviour of the number of ions per unit time collected from a gas detector as a function of the applied voltage; the four regions portray different operation regimes of a gas detector. An ionization chamber operates in the region II. The constant trend indicates that all the ions produced by the passage of the radiation are collected at the electrodes (saturation). Each of the three different curves corresponds to a particular type of particle: α: heavy particles; β: light particles, including electrons and positrons; γ: photons

performed with the same accuracy typical of other clinical beams. As mentioned earlier, the laser-driven acceleration systems are characterized by a very high dose rate. The correction factor for the ion recombination could be underestimated when applying the correction methods recommended in international protocols, because of the high charge density which would be produced in the volume of the chamber for each radiation pulse [18, 19]. Therefore measurements performed with ionization chambers could include a source of error due to the ion recombination in the sensitive volume of the ionization chamber. This problem has been addressed over the years [19–21]; as for now, with an appropriate correction on the ion recombination it is possible to perform measurements of absolute dosimetry with the ionization chambers even in the case of high dose rate clinical accelerator (dose rate $\sim$cGy/pulse). An example of a commercial ionization chamber used for absolute dosimetry in the clinical practice is shown in Fig. 9.7.

To date, however, there are no clinical accelerators with dose rate comparable to that of a laser-driven accelerator. In this case, more detailed studies will be required regarding the coefficients of ion recombination in order to correct the measurement of the ionization chamber appropriately. However, the ionization chamber has been used for measurements of relative dosimetry, in order to control the delivered dose of biological samples irradiated with laser-driven systems [17, 22, 23]. Indeed, the ionization chamber enables to observe the accumulated dose in real time, so that the effects of the fluctuations of the electron beam can be monitored. The measurements carried out with the ionization chamber should take into account the uncertainties

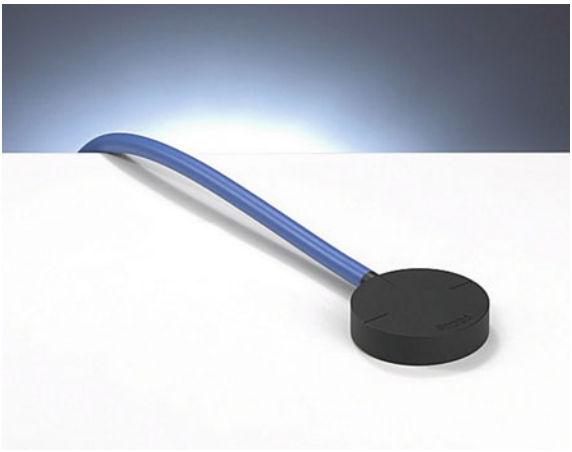

Fig. 9.7 A PTW ROOS electron chamber. This is a plane parallel chamber for dosimetry of high-energy electron beams in water and solid state phantoms

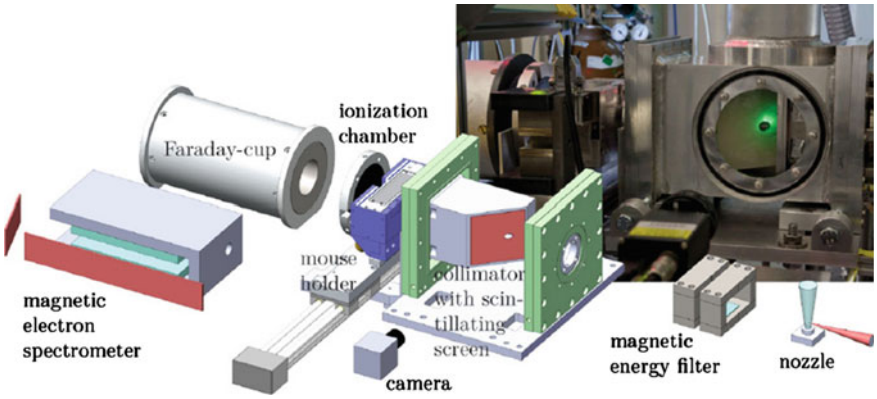

Fig. 9.8 Experimental setup used for radiobiology experiments with laser-driven electron beams in Jena. Figure credit: [17]

that arise from statistical errors, the fluctuations from shot to shot of the size of the radiation field, the beam intensity that could lead to effects of saturation. Figure 9.8 shows the experimental setup used for radiobiology experiments with laser-driven electron beams in a recent experiment carried out in Jena (Germany) and reported in [17]. In that experiment, an ionization chamber was used to measure the dose per pulse on a single-shot basis.

In case of laser-driven beams, measurements of relative dosimetry performed with the use of ionization chambers are generally supported by another detector, the Faraday cup.

9.2.3 *Faraday Cups*

The Faraday cup is an instrument to measure the current generated by an accelerated particle beam that runs through the cup. This current can in turn be used to determine the number of particles N that have entered the cup per unit area in a time t, using the simple relation $N = (1/A)\int_0^t (I/q)\mathrm{d}t$, where I is the measured current, A is the area of the beam and q is the charge carried by the particle [24]. A picture of a typical Faraday cup is shown in Fig. 9.9.

In order to retrieve the information on the absorbed dose from a Faraday cup measurement, different parameters have to be known: the beam area, the mass stopping power at a given specific energy, the energy spectrum of the particles, the total collected charge. A source of uncertainty related to measurements carried out with a Faraday Cup is the production of secondary electrons and positive ions from the interaction of the incident beam with the entrance window and with the metal surface of the cup. Indeed, the secondary particles may escape from the Faraday cup aperture. This would cause a wrong charge collection and can lead to an overestimate of the positive charge and to an underestimate of the electronic current [25, 26]. For these reasons, the use of the Faraday cup requires the knowledge of additional features of the specific accelerator used, such as the thickness of the entrance window, the guard ring, the type of vacuum, the size of the cup, the wall thickness and the material which it is made of.

A Faraday cup was also used as a detector, along with an ionization chamber and a magnetic spectrometer, in the experiment, carried out in Jena, cited above (see Fig. 9.8). Indeed, the Faraday cup provides the charge of the bunch by an average voltage per pulse multiplied by the number of pulses registered, thus obtaining a total voltage [22]. The variations in dose from shot to shot can be analyzed with the help of this detector in order to optimize, monitor and control the beam of accelerated particles. In this way the Faraday cup can be used to monitor the effective

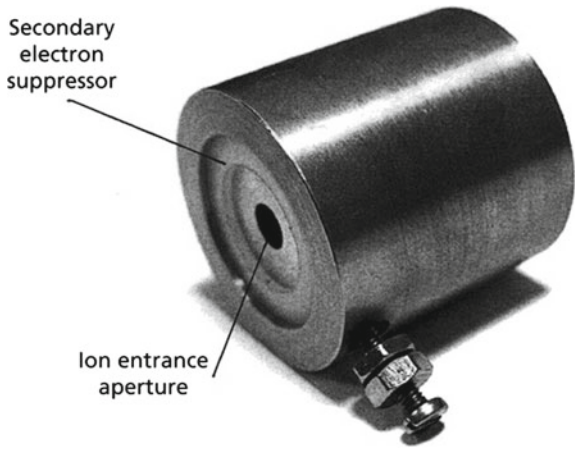

Fig. 9.9 A Faraday cup

bunch charge delivered [23]. These online dose measurement techniques are of a fundamental importance in view of the relatively higher shot-to-shot fluctuations affecting a laser-driven accelerator as compared to a conventional one.

Finally, it is worth mentioning that by comparing the dose values obtained using a Faraday cup with the ones retrieved by calibrated radiochromic films, absolute dosimetry can be carried out [17].

9.2.4 *Development of Dedicated Detectors: An Example*

Research is ongoing worldwide in order to develop novel detectors to cope with the peculiar features of laser-driven particle beams. As an example, we just mention here an innovative Faraday Cup recently designed and developed within the ELIMED collaboration. ELIMED (ELI-beamlines MEDical applications) is a collaboration between ELI-Beamlines researchers from Prague (Czech Republic) and an INFN-LNS (Laboratori Nazionali del Sud of the Istituto Nazionale di Fisica Nucleare) research group from Catania (Italy) aiming at demonstrating clinical applications of laser-driven proton beams (see [26]).

Preliminary studies were performed in order to optimize shape, dimensions, materials and the electric field of this Faraday cup. These studies have been carried out using modeling and simulation software and, also, the Monte Carlo GEANT4 simulation toolkit. To improve the overall charge collection efficiency of the Faraday cup, maximizing the charge collection accuracy, a special-shaped electric field has been designed. An asymmetric electric field characterized by a significant transverse component was used. This field is able to maximize the deflection of the secondary electrons generated by both the entrance window and the cup, thanks to the transverse component of the electric field (Fig. 9.10). This innovative detector was realized at INFN-LNS and preliminary experimental tests were recently carried out using the device shown in Fig. 9.11.

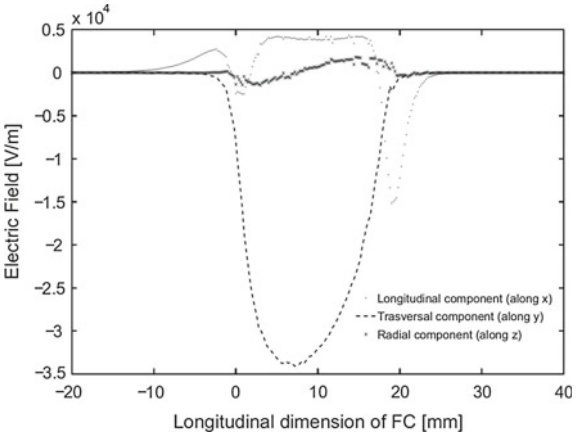

Fig. 9.10 Transverse, longitudinal and radial components of the electric field of a Faraday cup. Figure credit: [26]

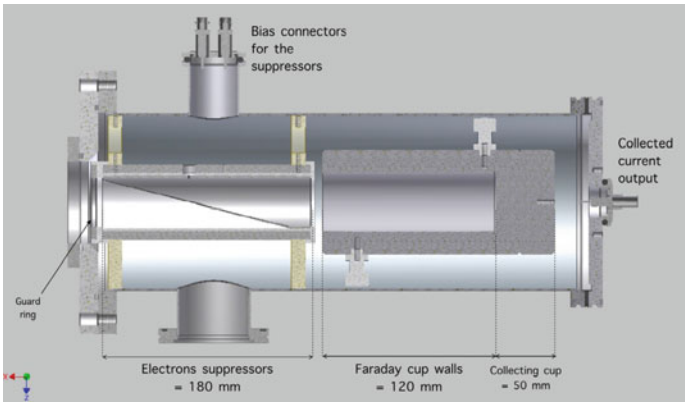

Fig. 9.11 Schematic layout of a Faraday Cup detector. The current collected in the cup is sent to an electrometer for integration. Figure credit: [26]

9.3 Dosimetric Simulations with Monte Carlo Methods

Monte Carlo simulations allow the study of new strategies and methodologies both in diagnostics and in therapy, making it possible to evaluate available techniques and to plan treatments that require mapping of appropriate dose. The Monte Carlo method is the most accurate and detailed calculation method in various fields of medical physics; for instance, it is used in the field of diagnostic imaging in radiology and nuclear medicine, in radiotherapy [for the accurate calculation of dose distributions and for the validation of the Treatment Planning System (TPS)], and for radioprotection studies. Monte Carlo applications can simulate complex models and a variety of physical processes on a wide range of energy and trace the path of each particle in volumes of different materials. The simulations can represent the geometry of the acceleration system reproducing the sizes, the shapes of the experimental set-up and the materials they are made of. For all these reasons, Monte Carlo simulations represent an important instrument to validate the dosimetric characterization of the beam.

A code that is widely used for medical physics studies is GEANT4 [27, 28]. It is a toolkit for the simulation of the interaction of radiation with matter which is able to potentially taking into account all the physical processes that involve the single particle that passes through the medium. Depending on the energy of the particles, the code can simulate, among others, the following physical processes: for photons, the production of electron/positron pairs, the Rayleigh and Compton scattering and the photoelectric effect; for electrons, energy loss due to ionization of the matter, pair production and *Bremsstrahlung* radiation; for hadrons, ionization, multiple scattering, nuclear scattering and fission.

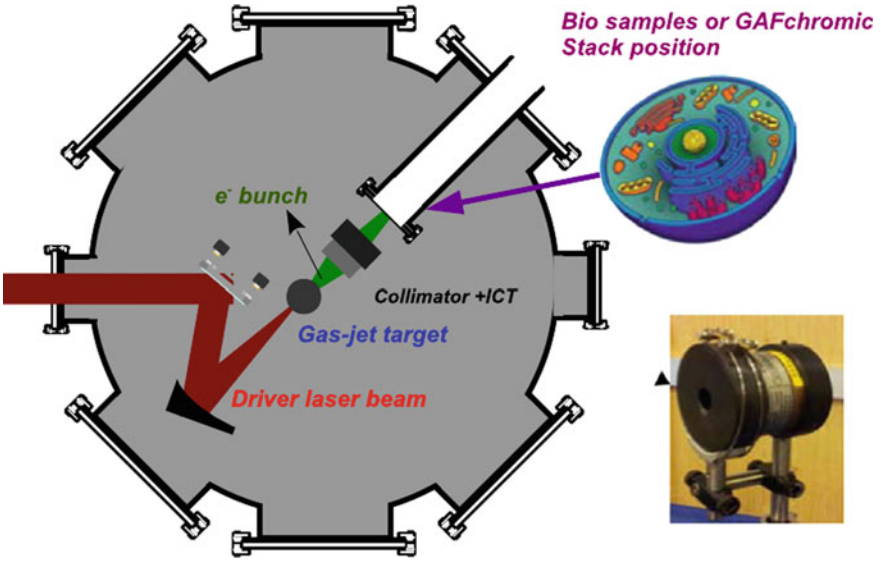

Fig. 9.12 Schematic view of the experimental setup used in the radiobiology experiments carried out at the ILIL-INO-CNR lab in Pisa, Italy

Generally speaking, Monte Carlo simulation techniques are the only method which can be applied in complex geometries for a wide range of energy and can provide a faithful simulation of the physical reality. As a general rule, the number of initial particles to be simulated depends upon the energy distribution that describes the source. Both the initial particles and the ones produced during the simulations are propagated geometrically in each volume for distances which depend upon the cross sections of the different processes the particle can undergo.

As said above, the GEANT4 toolkit is a valuable tool to study a typical laser-driven accelerator. Recently, an ad hoc tool was developed, based on it, to simulate laser-driven electron accelerators used for radiobiology experiments. In particular, it allows a full dosimetric characterization to be obtained by comparison with experimental measurements. As an example, we will be briefly describing a first application aimed at evaluating the dose distributions as obtained using a laser-driven accelerator setup at the Intense Laser Irradiation Laboratory of the Istituto Nazionale di Ottica of CNR in Pisa, Italy. A schematic view of the experimental setup is shown in Fig. 9.12. The accelerator is based upon a 10 TW laser system, delivering up to 450 mJ energy pulses with a < 40 fs pulse duration. The beam was focused, using an *f*/10 OAP mirror, onto a 1.2 mm long N_2 gas-jet at an intensity of about 3×10^{18} W/cm^2. An acceleration regime was seeked for, basically by adjusting the gas backing pressure and the focal position, mainly aiming at producing relatively low (~ 10 MeV) energy electron beams, with a total charge per bunch as high as possible. This energy range was selected as it is close to the one used in conventional IOERT (see Table 9.1). The experimental setup

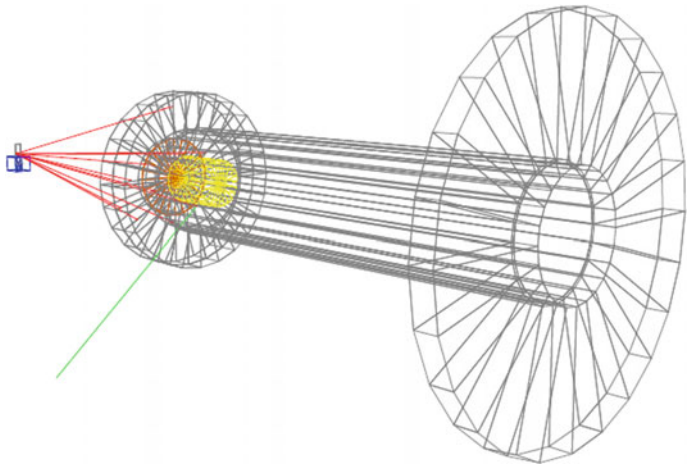

Fig. 9.13 Schematic of a typical laser-driven electron accelerator setup as simulated using GEANT4. The electron beam is generated at the gas-jet position. The sample is represented by the yellow mesh structure. Figure credit: [16]

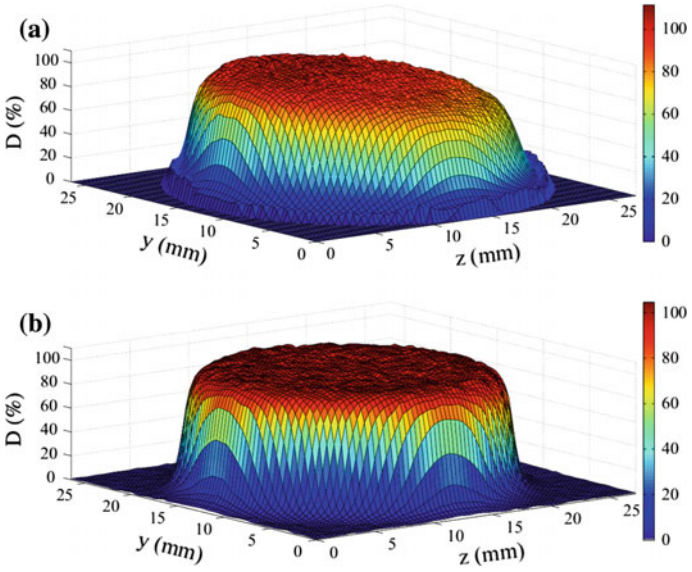

Fig. 9.14 **a** Measured dose profile measured using EBT3 gafchromic films. **b** Retrieved dose profiles of a laser-driven accelerator as provided by GEANT4 simulations. Figure credit: [16]

downstream of the "accelerator stage" (that is, the gas-jet nozzle) was optimized in order to carry out irradiation of in vitro samples for radiobiology studies. This involved, for instance, the usage of a cylindrical plastic tube to be used as a

collimator (as the ones used in an actual IOERT machine, see [5]) and a 100 μm thick kapton layer to act as a vacuum-air interface.

Figure 9.13 shows a sketch of the simulated setup, involving, among other elements, the electron source, an electron collimator and a vacuum-air interface. After the geometric reconstruction of the setup, the simulations can provide the energy lost at each position (identified by a voxel) by each particle created during the simulation. From such a kind of simulation, 2D and 3D distributions of the dose and PDD curves can be obtained. The data sets from simulations can also be compared with experimental measurements, carried out, for instance, using stacks of gafchromic films, to get informations on the energy and spatial distribution of the electron bunch from the source [16]. As an example, Fig. 9.14a shows the measured dose profile at the position of the biological samples to be irradiated. Figure 9.14 shows the corresponding profile as retrieved by a Monte Carlo simulation based on GEANT4.

9.4 Summary and Conclusions

In this chapter, we have briefly discussed the main issues related to the usage of "standard" dosimetric methods for the characterization of laser-driven electron beams. In particular, we have given an overview of the main devices used for the characterization of electron beams used in medical applications. From time to time, the main recommendations from international organizations supervising absolute dosimetry have also been briefly given. The issues possibly arising in the usage of techniques established for conventional accelerators for the dosimetry of ultrashort laser-driven beams have also been given whenever possible; these issues are mainly due to the very small duration of laser-driven electron beams, resulting in ultrahigh peak currents and dose rates.

As a conclusion, we stress that several issues have to be addressed before translating the usage of laser-driven beams into the clinical practice. From the point of view of the beam characterization, the possible errors due to the shot-to-shot stability, the beam homogeneity and symmetry and the dosimeter response have not to exceed standard percentage figures suggested by the recognized international dosimetry protocols. This seems currently a pretty challenging task. In general, the absolute dosimetric measurements would have to be carried out with dosimeters already in use in the clinical practice, such as ionization chambers and Fricke dosimeters (see [29] and references therein). On the other hand, the response of such devices at the very high dose rates featuring laser-driven particle beams have to be deepened as a preliminar step.

One of the key issues to be implemented in practice concerns the need of an active dose control using monitor chambers. The dose delivered by a clinical accelerator in a typical radiotherapy treatment at a specific depth with a given radiation field is expressed in monitor units. In general, two ionization chambers are used as monitor chambers in order to assess the delivered dose and to stop the beam when the prescribed monitor units have been reached.

Finally, we mention here that, unless advanced physical schemes not easily viable in a medical environment were used, current laser-driven particle beams feature a broad energy spectrum; this would possibly require an energy selection device to be used, whose insertion would in general affect the choice and/or behaviour of the device used for the dosimetric characterization.

Acknowledgements L.L. wishes to acknowledge support from the Italian Ministry of Health through the Project No. GR-2009-1608935 (Study of Radiobiological and Radiotherapic Effects of a Novel Laser-Driven Electron Accelerator, D.I. AgeNaS), from the CNR funded Italian research Network ELI-Italy (Attoseconds) and from the PRIN project (Contract No. PRIN2012AY5LEL). He also acknowledges contribution from the MIUR-FIRB project SPARX (Sorgente Pulsata Auto-Amplificata di Radiazione X) and the INFN Plasma-med collaboration. D.L. and G.R. acknowledge support from the project "IMINET—Italian Molecular Imaging Network".

References

1. L. Labate et al., Proc. SPIE **8778**, 87790O (2013)
2. L.A. Gizzi et al., Appl. Sci. **3**, 559–580 (2013)
3. E. Esarey et al., Rev. Mod. Phys. **81**, 1229 (2009)
4. J. van Tilborg et al., Phys. Rev. Lett. **96**, 014801 (2006)
5. S. Righi et al., J. Appl. Clin. Med. Phys. **14**, 6–18 (2013)
6. J. M. Schippers, M. Seidel, Phys. Rev. Spec. Top. - Accel. Beams **18**, 034801 (2015)
7. V. Malka et al., Mut. Res./Rev. Mut. Res. **704**, 142–151 (2010)
8. Sordina IORT Technologies S.p.A. website: http://soiort.com/en/
9. International Atomic Energy Agency, *Absorbed Dose Determination in External Beam Radiotherapy: An International Code of Practice for Dosimetry Based on Standards of Absorbed Dose to Water*. IAEA Technical Reports Series no. 398 (IAEA, Vienna, 2000)
10. A.S. Beddar et al., Med. Phys. **33**, 1476–1489 (2006)
11. P.R. Almond et al., Med. Phys. **26**, 1847–1870 (1999)
12. C. Fiandra et al., Med. Phys. **35**, 5463–5470 (2008)
13. A. Niroomand-Rad et al., Med. Phys. **25**, 2093–2115 (1998)
14. http://www.tecnologieavanzate.com/
15. V. Casanova Borca et al., J. Appl. Clin. Med. Phys. **14**(2), 2013
16. D. Lamia et al., Nucl. Instrum. Meth. Phys. Res. A **786**, 113–119 (2015)
17. M. Nicolai et al., Appl. Phys. B **116**, 643–651 (2014)
18. A. Piermattei, Phys. Med. Biol. **45**, 1869–1883 (2000)
19. J.W. Boag, E. Hocchäuser, O.A. Balk, Phys. Med. Biol. **41**, 885–897 (1996)
20. R.F. Laitano et al., Phys. Med. Biol. **51**, 6419 (2006)
21. F. Di Martino et al., Med. Phys. **32**, 2204–2210 (2005)
22. E. Beyreuther et al., Med. Phys. **37**, 1392–1400 (2010)
23. C. Richter et al., Rad. Meas. **46**, 2006–2009 (2011)
24. B. Schmidt, K. Wetzig, *Ion Beams in Materials Processing and Analysis* (Springer, 2013)
25. C. Richter et al., Phys. Med. Biol. **56**, 1529–1543 (2011)
26. G.A. Cirrone et al., Nucl. Instrum. Meth. Phys. Res. A **796**, 99–103 (2015)
27. S. Agostinelli et al., Nucl. Instrum. Meth. Phys. Res. A **506**, 250–303 (2003)
28. J. Allison et al., IEEE Trans. Nucl. Sci **53**, 270–278 (2006)
29. L.J. Schreiner, J. Phys: Conf. Ser. **3**, 9–21 (2004)